HHS Public Access

Author manuscript

Proc SPIE Int Soc Opt Eng. Author manuscript; available in PMC 2015 August 27.

Published in final edited form as:

Proc SPIE Int Soc Opt Eng. 2015 February 7; 9362: . doi:10.1117/12.2086866.

Preliminary results of non-contact THz imaging of cornea

Shijun Sung[a], **James Garritano**[b], **Neha Bajwa**[b], **Sophie Deng**[c], **Jean-Pierre Hubschman**[c], **Warren S. Grundfest**[a,b,d], and **Zachary D. Taylor**[b,d]

[a]Dept. of Electrical Engineering, UCLA, 420 Westwood Plaza, Los Angeles, CA, USA 90095

[b]Dept. of Bioengineering, UCLA, 420 Westwood Plaza, Los Angeles, CA, USA 90095

[c]Dept. of Ophthalmology, UCLA, 200 UCLA Medical Plaza, Los Angeles, CA, USA 90095

[d]Dept. of Surgery, UCLA, 200 UCLA Medical Plaza, Los Angeles, CA, USA 90095

Abstract

This paper presents a novel THz optical design that allows the acquisition of THz reflectivity maps of *in vivo* cornea without the need for a field flattening window and preliminary imaging results of in vivo rabbit cornea. The system's intended use is to sense small changes in corneal tissue water content (CTWC) that can be precursors for a host of diseases and pathologies. Unique beam optics allows the scanning of a curved surface at normal incidence while keeping the source detector and target stationary. Basic system design principles are discussed and image sets of spherical calibration targets and corneal phantom models are presented. The presented design will enable, for the first time, non-contact THz imaging of animal and human cornea.

Keywords

THz medical imaging; quasioptics; optical design

I. INTRODUCTION

Recent research in terahertz (THz) medical imaging suggests that active, standoff sensing systems based on THz frequency illumination may be ideal for mapping the distribution and movement of water near the surface of physiologic tissues [1–6]. The tissue of the cornea offers a unique opportunity for tissue water content (TWC) mapping due to its extreme homogeneity and low physiologic variation when compared to all other tissue systems in the human body [7]. Many diseases and pathologies such as Fuchs' dystrophy [8], keratoconus [9, 10], and corneal graft rejection [11] are defined by, proceeded by, or correlated with changes in corneal tissue water content (CTWC) and current clinical measurement methodologies do not allow for sufficiently early detection of these conditions [12].

One currently unavoidable aspect of THz medical imaging is the use of dielectric windows to flatten the imaging field. Most THz imaging optical designs employ off-axis parabolic (OAP) mirrors as they offer a very broad range of numerical apertures from a single element

Correspondence to: Zachary D. Taylor.

and exhibit dispersion free operation. The drawback of OAP mirror trains are their poor tolerance to angled for curved target surfaces thus the need for dielectric windows flatten the field. These windows are typically applied with slight, contact pressure, and create a specular, three layer system (air, dielectric window that isolates variations in receiver power to spatial variations in the tissue's intrinsic reflectivity.

In our recently published work we reported on the results of an *in vivo* rabbit cornea imaging trial [13, 14] where a protocol was employed to perturb corneal water content and a 12.7 μm thick Mylar window was utilized to enable millimeter wave sensing of tissue water content and companion THz imaging of corneal water content. Positive, correlations were observed between the acquired millimeter wave reflectivity and central corneal thickness (CCT) which is currently used as a screening tool for tissue water content variation. No statistically significant correlation was observed between the THz reflectivity and CCT measurements. Electromagnetic modeling and data analysis revealed that the protocol perturbed the thickness of the cornea but did not markedly perturb the water content. It was determined that the discrepancy in millimeter wave and THz reflectivity trends arose from a cavity affect where the ensemble of longitudinal modes at millimeter wave frequencies produced an increase in reflectivity for an increase in corneal thickness paired with a constant tissue water content while the THz reflectivity likely exhibited, under the same physiologic conditions, a slight oscillation in reflectivity whose peak-to-peak amplitude was below the noise limited sensitivity of the system. The variation in thickness was most likely the result of the contact pressure applied by the dielectric window.

The results of this experiment suggest that accurate, clinically relevant measurements of corneal water content using THz illumination, must be performed non-contact. This requirement requires a rethinking of the standard THz medical imaging optical design problem as the commonly employed technique of mapping a point source to a point on a planar target plane a point at the detector plane is not compatible with the imaging of spherical surface image.

In this paper we present a THz corneal imaging system design that uses planar mirrors, raster scanned on a planar, rectilinear grid, to scan the surface of a spherical target by sampling the aperture of a large OAP mirror with the collimated THz beam. The source and detector are collocated with a beam splitter thus enabling efficient image acquisition while the source, detector, and cornea remain stationary.

II. Clinical Corneal Water Content Sensing

The cornea is the outermost structure of the eye (Figure 1(a)) and displays an average thickness in humans of ~ 580 μm [15]. The normal water content of the cornea is closely related to its visible wavelength (400 nm – 700 nm) transparency and refractive capabilities and typically contains ~ 78% water by volume [15]. It plays the leading role in collecting and focusing light on the retina, and provides 46 of the average 59 total diopters of refractive power in the eye [16]. Currently available practice limits the *in vivo* measurement of corneal tissue water content to extrapolation using the central corneal thickness (CCT) measurements usually performed with ultrasound or optical coherence tomography (OCT)

based pachymetry where a probe is placed by a clinician on the apex of the cornea (Figure 1(b)) [12].

Corneal pachymetry operates on the assumption of a monotonically increasing relationship between CCT and the average water content of the cornea [18]. This relationship was established in 1965 from the empirical fit of 11 healthy *ex vivo* human corneas from a cornea bank and deviations of 20% or greater are seen in the data [17] (Figure 1(c)). Additionally, the model does not account for physiologic corneal thickness variation [15]. The water-content-mass relationship discussed in [17, 18] can be rewritten as a function of CCT as [13]:

$$H=\frac{m_{H20}}{m_{H20}+m_{dry}}=\frac{CCT-0.091}{CCT+0.051} \quad (1)$$

A plot of equation (1) is displayed in Figure 1(d) where shaded area spans the physiologic range of thicknesses observed in healthy cornea and the dotted line is a linear fit to equation (1) within the physiologically relevant range (shaded region) with an approximate slope of 40%/mm.

Two key issues are evident. First, the current techniques used to measure water content are indirect and, while intrinsically somewhat sensitive to changes in corneal tissue water content, cannot be used to perform absolute measurements of tissue water due. Thus they are, at best, a screening tool and not a diagnostic. Second, while pachymetry is an indirect measurement of corneal tissue water content, it is considered the gold standard in clinical practice thus the performance of new modalities must be evaluated in the context of CCT measurement. Any sensing modality, such as THz imaging through a dielectric window in contact with the cornea, must not markedly perturb the thickness of the cornea being imaged.

III. Optical Systems design

In this design, the cornea is positioned such that the center of the cornea is coincident with the focal point of a large OAP mirror as displayed in Figure 2(a). A collimated THz beam, parallel to the clear aperture optical axis, is then swept transverse across the clear aperture. The beam is incident on the parabolic mirror and is redirected and focused towards the mirror focal point. Due to the positioning of the cornea, this maintains normal incidence on the corneal surface throughout all possible transverse positions occupied by the collimated beam at the mirror clear apertures. This behavior results in the reflected beam retracing the path of the illumination beam and gives rise to the retrodirective nature of the design. The collimated beam position is controlled by the rectilinear scanning of two plat mirrors (a one dimensional representation if this is demonstrated in Figure 2(a)). To decouple the illumination and reflection beams the source and detector are optically co-located with a broad band beam splitter.

The key benefit of this configuration is that allows the source, detector, and target, to remain fixed thus enabling clinical evaluation in humans. There are two major detriments of this

configuration. (1) The beam splitter configuration results in a minimum of 6 dB optical path loss. Quasioptical characterization of the beam splitter used to obtain the results in the following section measured a beam splitter loss of ~ 8.5 dB. (2) The spot size on target is larger than the diffraction limited spot size because the focused illumination beam is intercepted by the cornea prior to the focal point. Further due to the lack of radial symmetry in the dimension of the OAP displayed Figure 2(a) the spot size varies across the surface of the cornea.

The source was a 650 GHz amplifier-multiplier chain (Virginia Diodes, VA) with ~1 mW output power. The multiplied chain was frequency modulated with a triangle wave at a rate of 10 kHz with an RF sweep bandwidth of ± 1.5 GHz. The source was also amplitude modulated with a square wave at a rate of 400 Hz. The detector was a zero-bias Schottky diode (Virginia Diodes, VA) mounted in a WR1.5 waveguide. The output of the detector was coupled to a lock in amplifier with a 1 ms time constant. Measurements were acquired at a rate of 30 Hz and were averaged together to obtain pixel values at the rate of ~ 2 Hz. The plane mirrors were translated with stepper motors

An image of a 6.5mm radius brass sphere is displayed in Figure 2(b) and Figure 2(c). Figure 2(b) is displayed with respect to the coordinates of the plane mirrors. The brass target nearly fills the clear aperture of the OAP and the abrupt drop in signal corresponds to the spatial limits of the clear aperture. The rectilinear coordinates of the image in Figure 2(b) are mapped to the corresponding spherical coordinates in Figure 2(c) where the orientation has been flipped in the vertical direction to align the image with the perspective of the individual operating the system (note the minimum signal within the clear aperture is at the top of Figure 2(b) and the bottom of Figure 2(c)).

IV. Contact lens drying

Over-the-counter soft contact lenses have been used previously as a phantom for corneal imaging due to their relevant geometry, water content, and material refractive index [19]. In this experiment a contact lens removed from its saline storage solution, mounted on a 6.5 mm radius polypropylene ball positioned at the focal point of the large OAP, and imaged over the course of 30 minutes as it was drying in ambient conditions. Three images in the time series separated by 10 minutes are displayed in Figure 3.

The reflectivity of the contact lens generally displayed a noticeable reduction starting from the outer rim of the lens and moving inward while the drop in lens center reflectivity is slower. This result is similar to what has been observed previously where the cornea loses water from the periphery faster than the center [19].

While the global dynamic contrast is congruent with what we have observed previously in experiments using a broadband, pulsed THz imaging system, there were noticeable areas where the contrast did not demonstrate a negative reflectivity trend vs time. Between the 0 and 10 minute marks the center reflectivity has increased while the periphery has generally decreased. Further, the reflectivity of the top right corner of the field of view demonstrated an increase as a function of time. We hypothesize that this is an etalon effect arising from the narrowband nature of the illumination and the wavelength order thickness of the contact

lens. As the lens dries it is possible that (1) the drop in water content results in a reduction of path loss concomitant with a modulation of thickness resulting in a modulation of optical path length and interference from destructive to constructive. Simultaneous, co-registered thickness maps of the cornea will help thoroughly explore this effect

V. Porcine eye

Visible and THz images of an ex vivo porcine eye are shown in Figure 4(a) and Figure 4(b) respectively. Fresh porcine eyes (Sierra Medical, CA) were gently wetted to re-hydrate post-mortem cornea surface then imaged for 30 minutes. Precise placement of the specimen was more difficult with the whole eye because the effective center of curvature of the cornea surface was difficult to ascertain. The eye was placed in a custom polymer mount and positioned in front of the large system OAP (Figure 4(a)).

A trend similar to that observed in the contact lens imaging experiments, was observed in the porcine eye imaging experiment. However, the porcine eye demonstrated a much more uniform the drying behavior throughout the probed corneal surface and no apparent spatial shift in image peak intensity. Further, there were no discernable etalons, which was expected due to the increased thickness of porcine cornea (~ 1 mm) as compared to human cornea (~ 550 μm) and the remaining tissue water content in tissue adjacent to back layer of the cornea that likely prevented the entire thickness of the cornea from drying out and limited the drying dynamics to the top surface. We believe that these THz images are the first ever reported of an intact, *ex vivo* cornea.

VI. Conclusion

A novel, optical THz imaging system was presented that can image a cornea (spherical target) while keeping the source, detector, and target stationary. The system scans the transverse position of a collimated beam in the clear aperture of a large OAP and maps this to an ensemble of focused beam angles at the focal point of the OAP mirror. By positioning the center of curvature of the cornea coincident with the focal point of the mirror the beam is incident normally across the surface of the cornea resulting in the retro-directive behavior of the design and enabling system methodology that is compatible with the requirements of *in vivo* imaging.

Acknowledgments

This work is supported by the National Eye Institute (NEI) Grant# R01EY021590 and the National Institute of Biomedical Imaging and Bioengineering (NIBIB) Grant# R21EB015084 and Grant# R21EB016896.

References

1. Ferguson B, Wang S, Gray D, Abbott D, Zhang XC. Identification of biological tissue using chirped probe THz imaging. Microelectronics Journal. 2002; 33:1043–1051.
2. Han PY, Cho GC, Zhang XC. Time-domain transillumination of biological tissues with terahertz pulses. Opt Lett. 2000; 25:242–244. [PubMed: 18059842]
3. L?ffler T, Bauer T, Siebert K, Roskos H, Fitzgerald A, Czasch S. Terahertz dark-field imaging of biomedical tissue. Opt Express. 2001; 9:616–621. [PubMed: 19424298]

4. Ferguson B, Wang S, Gray D, Abbot D, Zhang XC. T-ray computed tomography. Opt Lett. 2002; 27:1312–1314. [PubMed: 18026434]
5. Arnone, DD.; Ciesla, CM.; Corchia, A.; Egusa, S.; Pepper, M.; Chamberlain, JM., et al. Applications of terahertz (THz) technology to medical imaging. Munich, Germany: 1999. p. 209-219.
6. Hoshina, H.; Hayashi, A.; Miyoshi, N.; Fukunaga, Y.; Miyamaru, F.; Otani, C. Terahertz pulsed imaging of frozen biological tissues. Infrared, Millimeter, and Terahertz Waves; IRMMW-THz 2009. 34th International Conference on; 2009; 2009. p. 1-2.
7. Taylor ZD, Singh RS, Bennett DB, Tewari P, Kealey CP, Bajwa N, et al. THz Medical Imaging: in vivo Hydration Sensing. Terahertz Science and Technology, IEEE Transactions on. 2011; 1:201–219.
8. Adamis AP, Filatov V, Tripathi BJ, Tripathi RAmC. Fuchs' endothelial dystrophy of the cornea. Survey of Ophthalmology. Sep.1993 38:149–168. [PubMed: 8235998]
9. Krachmer JH, Feder RS, Belin MW. Keratoconus and related noninflammatory corneal thinning disorders. Survey of Ophthalmology. Jan.1984 28:293–322. [PubMed: 6230745]
10. Rabinowitz YS. Keratoconus. Survey of Ophthalmology. Jan.1998 42:297–319. [PubMed: 9493273]
11. Panda A, Vanathi M, Kumar A, Dash Y, Priya S. Corneal Graft Rejection. Survey of Ophthalmology. Jul.2007 52:375–396. [PubMed: 17574064]
12. Lackner B, Schmidinger G, Pieh S, Funovics MA, Skorpik C. Repeatability and reproducibility of central corneal thickness measurement with Pentacam, Orbscan, and ultrasound. Optom Vis Sci. Oct.2005 82:892–9. [PubMed: 16276321]
13. Taylor ZD, Garritano J, Sung S, Bajwa N, Bennett DB, Nowroozi B, et al. THz and mm-Wave Sensing of Corneal Tissue Water Content: Electromagnetic Modeling and Analysis. Terahertz Science and Technology, IEEE Transactions on. 2015; 5:170–183.
14. Taylor ZD, Garritano J, Shijun S, Bajwa N, Bennett DB, Nowroozi B, et al. THz and mm-Wave Sensing of Corneal Tissue Water Content: In Vivo Sensing and Imaging Results. Terahertz Science and Technology, IEEE Transactions on. 2015; 5:184–196.
15. Doughty MJ, Zaman ML. Human Corneal Thickness and Its Impact on Intraocular Pressure Measures: A Review and Meta-analysis Approach. Survey of Ophthalmology. Mar.2000 44:367–408. [PubMed: 10734239]
16. Gullstrand, A. Appendix. In: Helmholtz, Hv, editor. Handbuch der physiologischen Optik. Vol. 1. New York: Dover; p. 351-352.
17. Ytteborg J, Dohlman CH. Corneal Edema and Intraocular Pressure: II. Clinical Results. Arch Ophthalmol. Oct 1.1965 74:477–484. [PubMed: 5294510]
18. Brugin E, Ghirlando A, Gambato C, Midena E. Central Corneal Thickness: Z-Ring Corneal Confocal Microscopy Versus Ultrasound Pachymetry. Cornea. 2007; 26:303–307.10.1097/ICO.0b013e31802e1dea [PubMed: 17413957]
19. Bennett DB, Taylor ZD, Tewari P, Singh RS, Culjat MO, Grundfest WS, et al. Terahertz sensing in corneal tissues. Journal of Biomedical Optics. 2011; 16:057003–057003. [PubMed: 21639581]

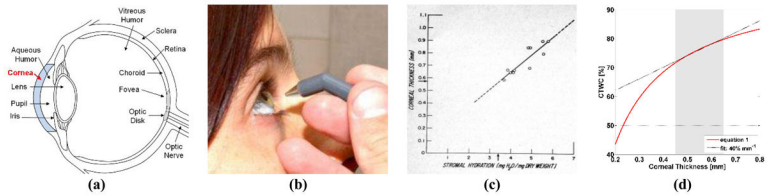

Figure 1.

Clinical corneal water content sensing. (a) Ocular anatomy, (b) Application of corneal pachymetry probe. (c) empirically derived relationship between thickness and water content [17]. (d) Conversion from water mass fraction to water content as a function of central corneal thickness.

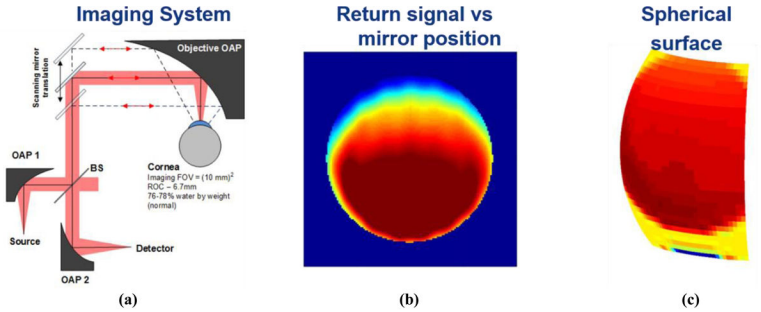

Figure 2.

THz imaging experiment set-up for imaging of spherical ocular surface. (a) System design. (b) Image of brass ball characterization target with respect to planar mirror position. (c) Re-mapping of THz image to corresponding target surface map.

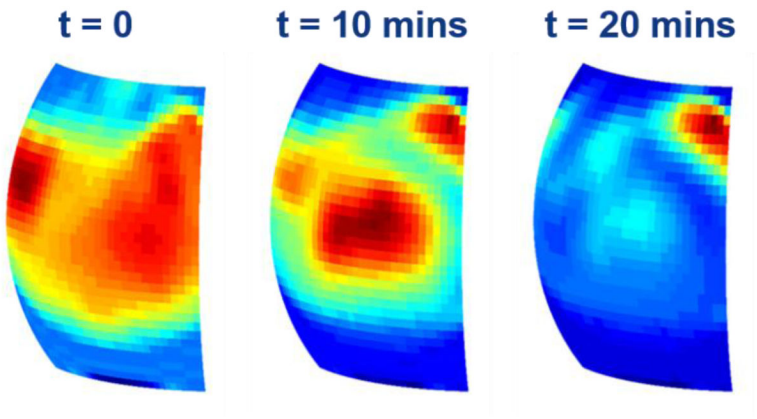

Figure 3.
THz image series of a drying contact lens

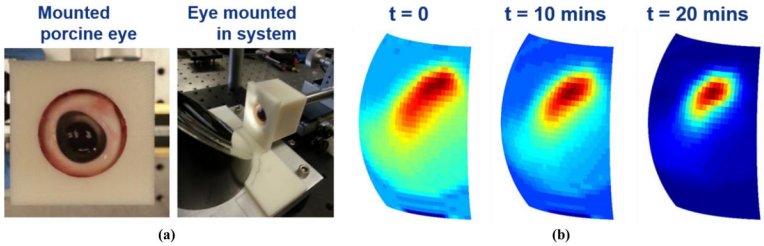

Figure 4.

THz imaging of a porcine eye (a) Mounted ex vivo porcine eye. (b) THz image series of the drying porcine eye